


COMMUNICATION

Kir4.1/Kir5.1 channels possess strong intrinsic inward rectification determined by a voltage-dependent K⁺-flux gating mechanism

Leticia G. Marmolejo-Murillo^{1*}, Iván A. Aréchiga-Figueroa^{2*}, Eloy G. Moreno-Galindo³, Tania Ferrer³, Rodrigo Zamora-Cárdenas³, Ricardo A. Navarro-Polanco³, José A. Sánchez-Chapula³, and Aldo A. Rodríguez-Menchaca^{3,4} 

Inwardly rectifying potassium (Kir) channels are broadly expressed in both excitable and nonexcitable tissues, where they contribute to a wide variety of cellular functions. Numerous studies have established that rectification of Kir channels is not an inherent property of the channel protein itself, but rather reflects strong voltage dependence of channel block by intracellular cations, such as polyamines and Mg²⁺. Here, we identify a previously unknown mechanism of inward rectification in Kir4.1/Kir5.1 channels in the absence of these endogenous blockers. This novel intrinsic rectification originates from the voltage-dependent behavior of Kir4.1/Kir5.1, which is generated by the flux of potassium ions through the channel pore; the inward K⁺-flux induces the opening of the gate, whereas the outward flux is unable to maintain the gate open. This gating mechanism powered by the K⁺-flux is convergent with the gating of PIP₂ because, at a saturating concentration, PIP₂ greatly reduces the inward rectification. Our findings provide evidence of the coexistence of two rectification mechanisms in Kir4.1/Kir5.1 channels: the classical inward rectification induced by blocking cations and an intrinsic voltage-dependent mechanism generated by the K⁺-flux gating.

Introduction

Inwardly rectifying potassium (Kir) channels are an important class of cell membrane proteins that regulate membrane excitability, heart rate, vascular tone, insulin release, and K⁺ transport in epithelia and glia (Hibino et al., 2010). Kir channels are so named due to their characteristic I-V relationship, as they conduct large inward currents at potentials negative to the K⁺ equilibrium potential (E_K) and display a voltage-dependent decline of K⁺ conductance (rectification) upon membrane depolarization to potentials positive to E_K.

In mammals, 16 Kir subunit genes have been identified corresponding to 7 subfamilies (Kir1.x to 7.x), which exhibit different degrees of rectification, from strong (e.g., Kir2 and Kir3) to intermediate (e.g., Kir4) to weak (e.g., Kir1 and Kir6; Hibino et al., 2010; Swale et al., 2014). Cumulative evidence has established that inward rectification is caused by cytoplasmic cations, such as polyamines (spermine [SPM], spermidine, and putrescine) and Mg²⁺, which plug the conduction pathway after depolarization, thus limiting the K⁺ efflux (Vandenberg, 1987; Lopatin et al., 1994; Nichols and Lee, 2018). Several negatively charged residues along the conduction

pore of Kir channels have been proposed as binding sites for blocking cations (Stanfield et al., 1994; Kubo and Murata, 2001; Pegan et al., 2005). The first to be identified was a residue in the second transmembrane helices of Kir channel subunits. The strongly rectifying Kir2.1 contains a negatively charged residue (D172; called the rectification controller) at this position (Stanfield et al., 1994), whereas the weakly rectifying Kir1.1 has an uncharged amino acid (N171). Introducing a negative charge at this position in Kir1.1 channels (N171D) increases affinity for endogenous blockers, thereby increasing rectification (Lu and MacKinnon, 1994). Additionally, neutralization of acidic residues on the cytoplasmic pore of Kir channels (E224 and E299 in Kir2.1 channels) has been shown to affect the binding of endogenous blockers (Yang et al., 1995; Kubo and Murata, 2001). Recording of Kir2.1 and Kir4.1 currents in the absence of polyamines and Mg²⁺ (using the inside-out configuration) practically abolishes inward rectification, exhibiting quasi-linear I-V relationships (Fakler et al., 1994; Guo and Lu, 2002) and suggesting that no other mechanism of rectification exists in these channels.

¹Departamento de Medicina y Nutrición, División de Ciencias de la Salud, Universidad de Guanajuato, León, México; ²Consejo Nacional de Ciencia y Tecnología, Facultad de Medicina, Universidad Autónoma de San Luis Potosí, San Luis Potosí, México; ³Centro Universitario de Investigaciones Biomédicas, Universidad de Colima, Colima, México; ⁴Departamento de Fisiología y Biofísica, Facultad de Medicina, Universidad Autónoma de San Luis Potosí, San Luis Potosí, México.

*L.G. Marmolejo-Murillo and I.A. Aréchiga-Figueroa contributed equally to this paper; Correspondence to José A. Sánchez-Chapula: sancheza@ucol.mx; Aldo A. Rodríguez-Menchaca: aldo.rodriguez@uaslp.mx.

© 2021 Marmolejo-Murillo et al. This article is distributed under the terms of an Attribution–Noncommercial–Share Alike–No Mirror Sites license for the first six months after the publication date (see <http://www.rupress.org/terms/>). After six months it is available under a Creative Commons License (Attribution–Noncommercial–Share Alike 4.0 International license, as described at <https://creativecommons.org/licenses/by-nc-sa/4.0/>).

Homomeric Kir4.1 channels display intermediate inward rectification, which largely depends on the E158 residue (equivalent to D172 in Kir2.1 channels). The E158N mutation converts Kir4.1 channels into weaker rectifiers (Fakler et al., 1994). Kir4.1 can also form heteromeric channels with the silent Kir5.1 subunit, resulting in different rectification and kinetic properties, as well as pH sensitivity (Pessia et al., 1996). Although Kir5.1 contains a neutral residue in the position of the rectification controller (N161), heteromeric Kir4.1/Kir5.1 channels display stronger rectification than homomeric Kir4.1 channels, implying that another mechanism of rectification could exist. Therefore, the mechanism for inward rectification of Kir4.1/Kir5.1 channels is not completely understood yet, and deserves further investigation. In the present study, we show for the first time that heteromeric Kir4.1/Kir5.1 channels possess two mechanisms of inward rectification: the classical extrinsic rectification induced by polyamines and Mg²⁺ plugging the pore and a strong intrinsic voltage-dependent rectification, generated by a gating mechanism powered by the K⁺-flux.

Materials and methods

Cell transfection

Rat Kir4.1 in pEGFPC1 vector (Clontech) was a kind gift from Dr. Colin G. Nichols (Washington University, St. Louis, MO), and tandemly linked rat Kir4.1/Kir5.1 in pCDNA3.1 (+) vector (Invitrogen) was generously provided by Dr. Stephen J. Tucker (University of Oxford, Oxford, UK). Kir4.1 and Kir4.1/Kir5.1 cDNAs were expressed in HEK-293 cells (American Type Culture Collection; CRL-1573) by transient transfection with Lipofectamine 2000 reagent (Invitrogen). For macroscopic current recordings, cDNAs were transfected as follows: 15 ng (Kir4.1) and 300 ng (Kir4.1/Kir5.1) for experiments in whole-cell configuration and 1.5 μg (Kir4.1) and 2.5 μg (Kir4.1/Kir5.1) for inside-out configuration. Cells were maintained in Dulbecco's modified Eagle's medium (Gibco), supplemented with 10% FBS (Gibco) and 1% antibiotic-antimycotic solution (100 U penicillin, 100 μg streptomycin, and 0.25 μg amphotericin B per milliliter; Sigma-Aldrich) at 37°C in a humidified atmosphere of air-5% CO₂.

Patch-clamp recordings

Electrophysiological experiments were performed at room temperature (22–24°C) 24 h after the transfection of cDNAs. Macroscopic currents were recorded in both whole-cell and inside-out configurations of the patch-clamp technique (Hamill et al., 1981). Currents were filtered with a four-pole Bessel filter at 1 kHz and digitized at 10 kHz using an Axopatch 200B amplifier (Molecular Devices) driven by pClamp 9 software (Molecular Devices). Patch pipettes were pulled using a flaming/brown micropipette puller (Sutter Instrument Company) from borosilicate capillary glass (WPI). An agar-KCl bridge was used to ground the bath.

For whole-cell experiments, the bath was superfused with a solution containing (in mM) 130 NaCl, 4 KCl, 1.8 CaCl₂, 1 MgCl₂, 10 glucose, and 10 HEPES, adjusted to pH 7.4 with NaOH. The pipettes had a resistance of 2–3 MΩ when filled with (in mM) 110 KCl, 1 MgCl₂, 5 K₄BAPTA, 5 K₂ATP, and 10 HEPES, adjusted to pH

Table 1. Composition (in mM) of the FVPP solutions

Compound	Standard (K ⁺ 200)	K ⁺ 77	Compound	K ⁺ 19
KCl	123	—	KCl	19
K ₂ EDTA	5	5	Na ₂ EDTA	5
K ₂ HPO ₄	7.2	7.2	Na ₂ HPO ₄	7.2
KH ₂ PO ₄	8	8	NaH ₂ PO ₄	8
KF	5	5	NaF	5
K ₄ P ₂ O ₇	10	10	Na ₄ P ₂ O ₇	10
Na ₃ VO ₄	0.1	0.1	Na ₃ VO ₄	0.1
NaCl	—	123	NaCl	104

pH was adjusted to 7.2 with KOH (standard) or NaOH (K⁺ 77 and K⁺ 19).

7.2 with KOH. Series resistance and capacitance were compensated at ~80%.

For inside-out experiments, both the pipette and the bath solutions were the same, which was a fluoride, vanadate, and pyrophosphate (FVPP) solution (with no Mg²⁺ and SPM and containing 200 mM K⁺) that was used to prevent current rundown (Huang et al., 1998; Table 1). For recordings in the presence of different K⁺ concentrations to modify E_K (see Fig. 6), we first substituted all the potassium chloride (123 mM) by sodium chloride while maintaining the same other components to obtain a FVPP solution with 77 mM K⁺ (Table 1). This solution was used in the pipette or in the bath as required. To further lower the K⁺ concentration to a level where the same driving force conditions could be applied for an outwardly and inwardly K⁺ gradient, we considered that an E_K shift to –60 and +60 mV (total K⁺ gradient of ~120 mV) would be adequate; thereby, the required K⁺ concentration was 19 mM (see Table 1).

All solutions were continuously perfused using a rapid switcher device (SF-77B; Warner Instruments). Macroscopic currents are represented as the current sensitive to pH 5.0. This pH condition was sufficient to abolish any detectable current through Kir4.1 and Kir4.1/Kir5.1 channels.

Drugs

SPM was obtained from Sigma-Aldrich, dissolved in water as a 100-mM stock solution, and diluted in the bath solution just before use. Brain phosphatidylinositol 4,5-bisphosphate (PIP₂; dissolved in chloroform:methanol:water) was purchased from Avanti Polar Lipids, aliquoted, dried under a nitrogen stream, and stored at –80°C. Before the experiment, PIP₂ was dissolved in FVPP solution by sonication for 10 min to obtain a concentration of 10 μM. All other reagents were purchased from Sigma-Aldrich, except K₄BAPTA (Santa Cruz Biotechnology).

Data analysis

Data are presented as mean ± SEM (*n* corresponds to the number of cells or patches recorded from at least three different transfections). Recordings were analyzed using pClamp 10 (Molecular Devices) and Origin 8 (OriginLab Corp.) software. Nonlinear least-square kinetic analysis of activation and deactivation of currents was performed in accordance with a single- or a

double-exponential equation and based on the simplex algorithm. Where appropriate, paired or unpaired Student's *t* test or ANOVA was used for evaluating statistical difference. A two-tailed probability value of <0.05 ($P < 0.05$) was considered statistically significant.

Results

Kir4.1/Kir5.1 channels exhibit stronger inward rectification than Kir4.1 channels in whole-cell configuration

Using standard intracellular and extracellular solutions with an asymmetric (physiological) K^+ gradient (140 and 4 mM, respectively), we first evaluated HEK-293 cells expressing Kir4.1/Kir5.1 and Kir4.1 channels in the whole-cell configuration by means of a square-pulse voltage protocol. From a holding potential of -80 mV, 2-s test pulses were applied to voltages between -120 and 0 mV, with 10-mV increments every 10 s. Representative Kir4.1/Kir5.1 currents are shown in Fig. 1 A. Inward currents elicited at voltages negative to E_K exhibited a slow time-dependent increase that was more prominent at potentials below -100 mV. At potentials positive to E_K , the outward currents progressively decreased, reaching a steady state by the end of the pulse. The outward current decay was voltage dependent, increasing as the potential became more depolarized. This behavior induced a crossover of the outward currents at potentials above -50 mV (Fig. 1 A, inset). The I-V relationship measured at the end of the test pulses revealed a strong inwardly rectifying profile, clearly showing a negative slope conductance at potentials positive to -50 mV (Fig. 1 B).

By contrast, homomeric Kir4.1 channels exhibited inward currents with faster time-dependent increases (Fig. 1 C) than those observed in heteromeric Kir4.1/Kir5.1 currents. Additionally, outward currents showed a time-dependent decline, though the size of the currents at the end of the test pulses was always larger as the potential was more positive (Fig. 1 C). The I-V relationship showed that inward rectification of Kir4.1 currents was not as strong as that of heteromeric Kir4.1/Kir5.1 channels, and thus a negative slope was not present (Fig. 1 D).

Inward rectification of Kir4.1/Kir5.1 channels persists in the absence of endogenous blockers

Next, we assessed macroscopic Kir4.1/Kir5.1 and Kir4.1 currents in the absence of intracellular Kir blocking cations (Mg^{2+} and polyamines), that is, in the inside-out configuration. FVPP solution (see Materials and methods) was used on both sides of the membrane patches to prevent "rundown" of currents (Huang et al., 1998). Although Kir4.1/Kir5.1 currents were recorded after 3–5 min of exhaustive perfusion of the internal side of membrane patches with a rapid switcher device, the inward rectification of this channel persisted (even for up to 20–30 min). Thus, to characterize this apparent "intrinsic" inward rectification of Kir4.1/Kir5.1, we used a triple-pulse voltage protocol: from a holding potential of 0 mV, a 2-s hyperpolarizing prepulse to -140 mV was applied, followed by 2-s depolarizing test pulses to potentials between -140 and $+100$ mV (in 20-mV increments) before returning to -140 mV for 2 s. As depicted in Fig. 2 A, the pulse to -140 mV evoked a small instantaneous

inward current, followed by a slowly activating current that proceeded until a steady state was achieved. Depolarizations to the test pulses elicited instantaneous inward and outward currents with a driving force-induced variation of their amplitudes, and then currents decreased with a marked time and voltage dependence. Notably, outward currents were highly reduced, although a small K^+ efflux always remained. The subsequent hyperpolarization to -140 mV generated instantaneous inward currents whose amplitude varied with voltage (smaller as the previous test pulse was more depolarized), followed by the gradual reopening of channels to reach the same current level as that in the prepulse potential (Fig. 2 A). The I-V relationship measured at the end of the test pulses shows the strong inward rectification of Kir4.1/Kir5.1 channels, even in the absence of endogenous blockers (Fig. 2 B). By decreasing the EDTA concentration of the FVPP solution to 1 mM or increasing it to 10 mM, we obtained the same results as those using the standard 5-mM concentration of the FVPP control solution (Fig. 2, B–D). As observed in Fig. 2, A–D, it should be emphasized that the rectification occurred not only at positive voltages to E_K but also at the most negative voltages evaluated. These results imply that at the start of the test pulses the channels are initially activated (open), and then a time-dependent deactivation (closure) occurs.

In contrast, both inward and outward Kir4.1 currents induced by voltage were virtually time independent (Fig. 2 E), producing a linear I-V relationship similar to that expected of an ohmic conductor (Fig. 2 F). Thus, unlike heteromeric channels, macroscopic inside-out Kir4.1 currents exhibited nonrectifying behavior in the absence of endogenous blockers, as typical for Kir channels.

As Kir4.1/Kir5.1 channels displayed inward rectification in the absence of intracellular Kir blocking cations, we decided to explore whether exogenous SPM alters the rectification of these channels. Thus, we elicited macroscopic currents in the inside-out configuration by using the same triple-pulse voltage protocol as described for Fig. 2. As expected, SPM did not affect inward currents (in terms of either amplitude or time dependence), while a voltage-dependent block was evident at $+80$ and $+100$ mV (Fig. 3 A), thereby reducing further the current amplitude (Fig. 3 B) and accelerating its time-dependent decay (Fig. 3, C and D). Hence, despite having strong inward rectification, outward currents were still affected by SPM, implying that this polyamine is able to block the heteromeric channel. Alternatively, the inward rectification of inside-out Kir4.1 currents was restored after exposure to this polyamine (Fig. 3, E and F), as previously reported (Kucheryavykh et al., 2008), decreasing the channel conductance at positive potentials as a result of Kir4.1 block by SPM.

Overall, these results suggest that the inward rectification of Kir4.1/Kir5.1 channels involves two different mechanisms: the classical extrinsic rectification induced by endogenous blockers (Mg^{2+} and polyamines) and a strong intrinsic voltage-dependent rectification.

Activation and deactivation kinetics of Kir4.1/Kir5.1 channels

It is widely known that Kir channels do not possess a canonical voltage sensor. Thus, we investigated how voltage dependence

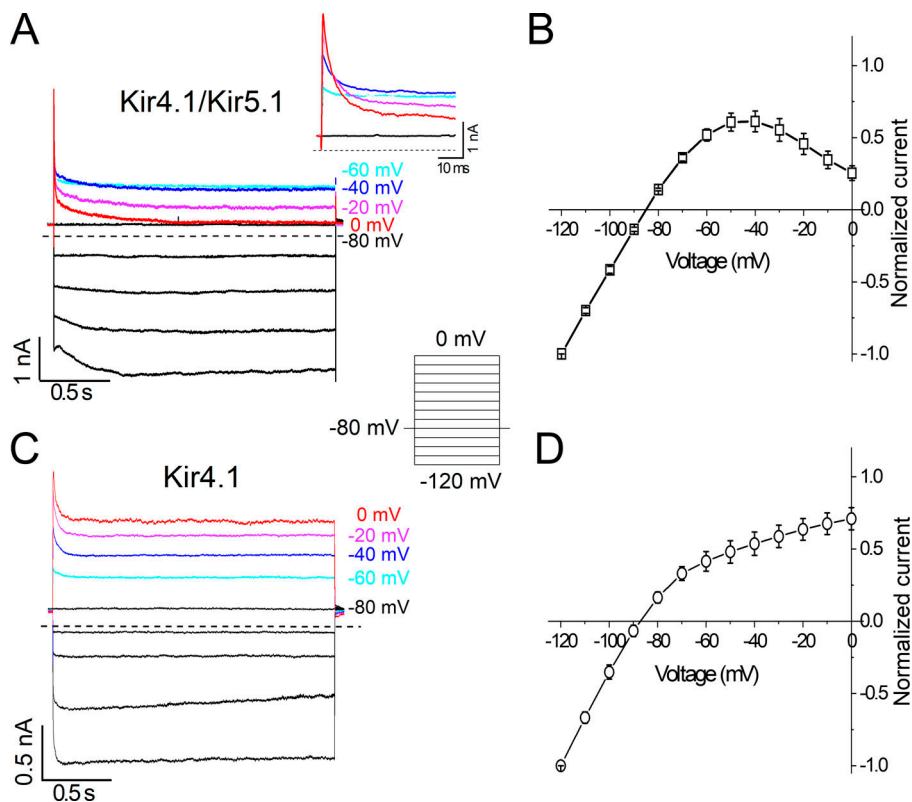


Figure 1. Inward rectification of Kir4.1 and Kir4.1/Kir5.1 channels in whole-cell control conditions. (A and C) Macroscopic whole-cell Kir4.1/Kir5.1 (A) and Kir4.1 (C) currents in HEK-293 cells. Currents were evoked by using the voltage-step protocol shown in the inset at the center of the four panels. For clarity, currents at potentials -70 , -50 , -30 , and -10 mV are not shown. The inset of A corresponds to the amplification of the first 50 ms of outward currents from this panel. The dashed line denotes the zero-current level. (B and D) Normalized I-V relationships for Kir4.1/Kir5.1 (B) and Kir4.1 (D) currents measured at the end of the test pulses and normalized to the amplitude of the current recorded at -120 mV. $n = 9$ (Kir4.1/Kir5.1) and $n = 6$ (Kir4.1).

arises in Kir4.1/Kir5.1 channels. First, we evaluated the kinetics of activation and deactivation of currents induced by voltage. From a holding potential of $+100$ mV (to promote channel closure), the activation kinetics was assayed by applying 2-s hyperpolarizing test pulses between $+100$ mV and -160 mV (with 20-mV decrements) to progressively open the channels. For potentials between $+100$ and -40 mV, outward and inward currents were evoked in a voltage-dependent but time-independent manner, whereas from -60 mV to more hyperpolarizing potentials, the amplitude of inward currents increased with voltage and time dependence (i.e., a gradual increase in current amplitudes was observed; Fig. 4 A). However, when these latter currents were fitted to a single exponential function to measure the rate of channel activation (τ_{act}), no significant difference was found at the analyzed potentials (Fig. 4 B; $P = 0.18$).

The deactivation process of the Kir4.1/Kir5.1 channels was examined by means of a hyperpolarized prepulse to -140 mV to open the channels, followed by test pulses from -120 to $+100$ mV (in 20-mV increments) to gradually deactivate the channels (Fig. 4 C). An important feature was that outward currents exhibited a high degree of deactivation (almost complete under this condition), whereas there was only partial deactivation of the inward currents; thus, we analyzed inward and outward currents separately. Currents generated with the test pulses were best fitted to a single (inward currents) or double (outward currents) exponential function to estimate the rate of channel closure (τ_{deact}). Similar to the activation kinetics, the deactivation kinetics of both inward and outward currents of the Kir4.1/Kir5.1 channels was not voltage dependent (Fig. 4 D; $P = 0.75$ for

inward currents, while for outward currents $P = 0.36$ and 0.82 for τ_{slow} and τ_{fast} , respectively). However, the fact that inward currents were best fitted to a single exponential and outward currents required a double exponential function suggests the presence of a voltage-dependent component in the deactivation process of Kir4.1/Kir5.1 currents.

PIP₂ largely reduces the intrinsic inward rectification of Kir4.1/Kir5.1 channels

There are several intracellular modulators of the gating of Kir channels, including the membrane-delimited anionic lipid, PIP₂, which induces conformational changes at the helix-bundle crossing to activate these channels. Consequently, the application of PIP₂ stabilizes the open state of the channel, increasing the amplitude of macroscopic currents (Rapedius et al., 2007). Therefore, we aimed to assess the effects of this compound on the Kir4.1/Kir5.1 intrinsic inward rectification mechanism by recording macroscopic inside-out Kir4.1/Kir5.1 currents in the presence of $10 \mu\text{M}$ PIP₂. Representative current traces of Kir4.1/Kir5.1 in the absence of and during perfusion of PIP₂ are shown in Fig. 5, A and B, respectively. Currents were elicited using the triple-pulse protocol described for Fig. 2. As depicted in Fig. 5 B, currents increased in the presence of PIP₂, and the inward rectification was strikingly reduced. Normalized I-V relationships for the currents measured at the end of the test pulses are shown in Fig. 5 C. With PIP₂, the relationship displayed an almost linear behavior, which contrasts with the strong inward rectification observed in these channels under control conditions. In addition, the effect of SPM ($10 \mu\text{M}$) was still appreciated after the application of PIP₂ (Fig. 5 D) by blocking outward

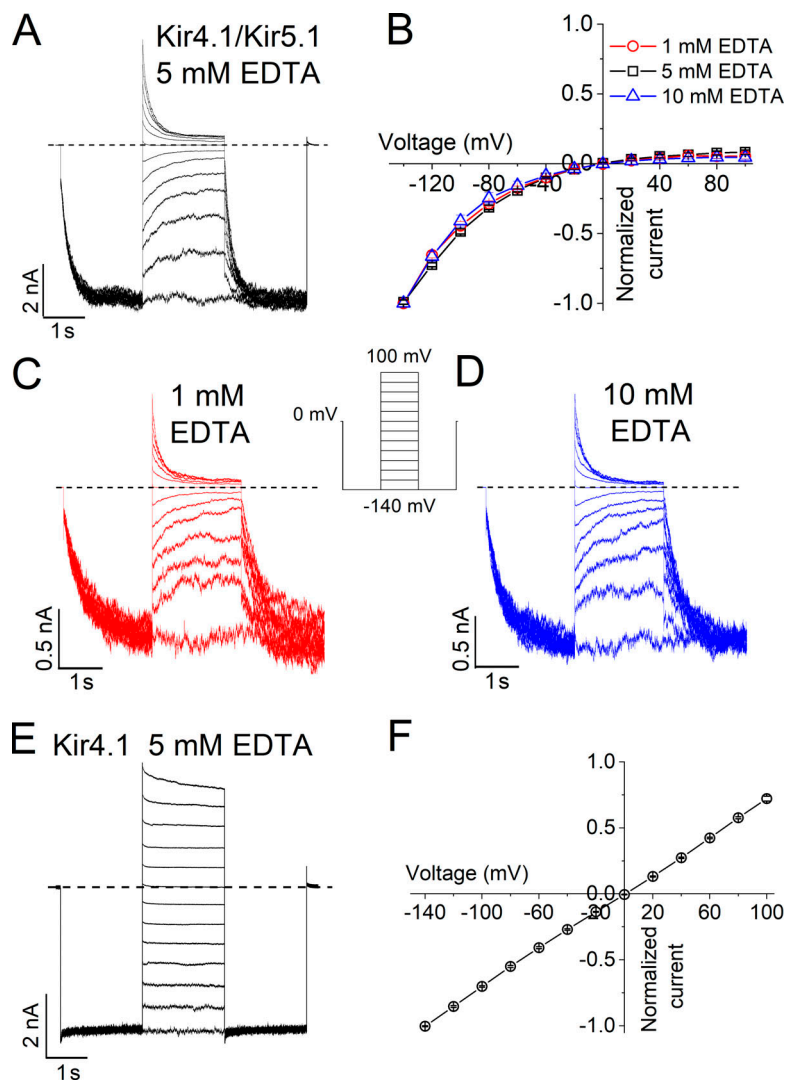


Figure 2. Heteromeric Kir4.1/Kir5.1 but not homomeric Kir4.1 channels inwardly rectify in inside-out configuration. (A–E) Representative macroscopic Kir4.1/Kir5.1 (A, C, and D) and Kir4.1 (E) currents recorded in the inside-out configuration when applying the triple-pulse voltage protocol depicted in the inset. The bath (intracellular) solution contained 5 mM (A and E), 1 mM (C), or 10 mM (D) EDTA. **(B and F)** Normalized I-V relationships for Kir4.1/Kir5.1 (B) and Kir4.1 (F) currents measured at the end of the test pulses and normalized to the amplitude of the current recorded at -140 mV. The dashed line denotes the zero-current level. $n = 6$ –8 cells for each channel and EDTA condition.

currents and had no effect on inward currents. This indicates that PIP_2 only disrupted the intrinsic rectification mechanism without affecting the extrinsic inward rectification mechanism.

A K^+ -flux gating mechanism underlies the intrinsic inward rectification of Kir4.1/Kir5.1 channels

Recently, the influence of potassium ions on the gating mechanism of ion channels with no voltage sensor was discovered (Kurata et al., 2010; Schewe et al., 2016). Thus, we next sought to investigate the role of these ions in the intrinsic inward rectification of Kir4.1/Kir5.1 channels. To this end, we modified E_K by changing the K^+ concentration (see Materials and methods) and performed similar experiments as described for Fig. 2, except that the prepulse potentials as well as the most depolarizing and hyperpolarizing test pulses were adjusted to compensate for the shift of E_K and thus assess currents under similar conditions of driving force (Fig. 6). From symmetrical K^+ concentrations (200 mM), inwardly rectifying currents were also evoked by both decreasing this ion (to 77 mM) in the extracellular (pipette) solution (Fig. 6 A) or in the intracellular (bath) solution (Fig. 6 C). Measuring currents at the end of the test pulses, the I-V relationships show that currents reversed very close to the

predicted E_K (-24 and $+24$ mV) and exhibited a parallel displacement in accordance with the shift of E_K (Fig. 6 D). We also estimated an index of rectification (calculated as the ratio between the outward and inward currents obtained with the most depolarizing and hyperpolarizing test pulses, respectively), which was used to evaluate the extent of inward rectification. Notably, despite the same driving force conditions, the current ratio was significantly modified depending on the direction of the K^+ gradient, $200 \text{ mM } \text{K}^+_{\text{int}}/77 \text{ mM } \text{K}^+_{\text{ext}}$ versus $77 \text{ mM } \text{K}^+_{\text{int}}/200 \text{ mM } \text{K}^+_{\text{ext}}$ (Fig. 6 E).

To corroborate this finding, we further decreased the K^+ concentration (to 19 mM; see Materials and methods and Table 1) in the extracellular (pipette; Fig. 6 F) or intracellular (bath) solution (Fig. 6 G), thereby changing the E_K to approximately -60 mV and approximately $+60$ mV, respectively. As expected, the I-V curves showed a higher displacement in accordance with the shift of E_K and a marked difference in the degree of inward rectification (Fig. 6 H). The current ratio of the outwardly directed K^+ gradient condition ($200 \text{ mM } \text{K}^+_{\text{int}}/19 \text{ mM } \text{K}^+_{\text{ext}}$) was 0.72 ± 0.13 , compared with 0.02 ± 0.006 for the inwardly directed K^+ gradient condition ($19 \text{ mM } \text{K}^+_{\text{int}}/200 \text{ mM } \text{K}^+_{\text{ext}}$; Fig. 6 I). In summary, these results indicate that the intrinsic inward

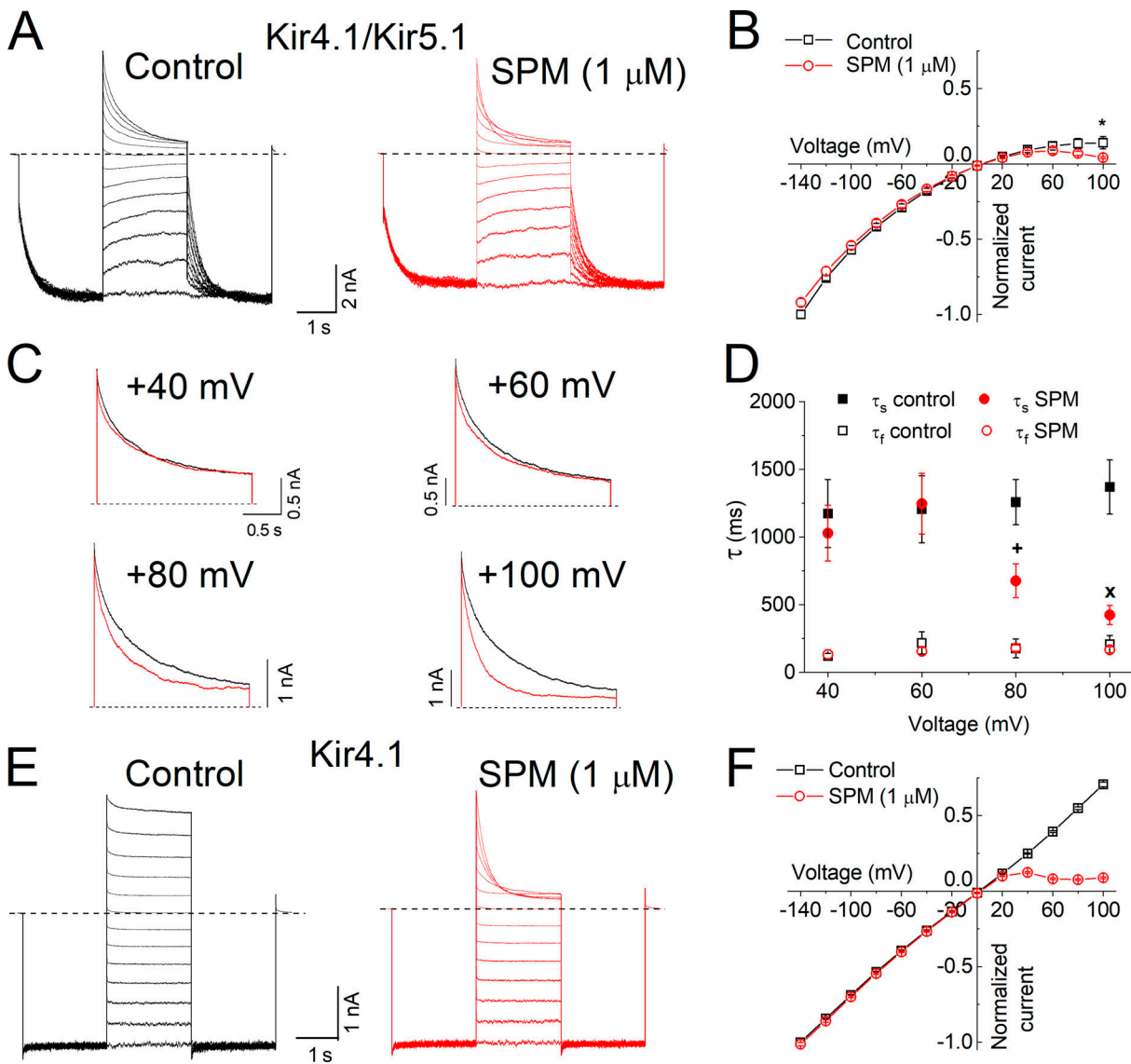


Figure 3. **Effect of exogenous SPM on inside-out Kir4.1/Kir5.1 and Kir4.1 currents.** (A) Kir4.1/Kir5.1 currents before (control) and after perfusing 1 μ M SPM in the bath. Currents were recorded in the inside-out configuration applying the same triple-pulse voltage protocol as for Fig. 2. (B) Normalized I-V relationships for Kir4.1/Kir5.1 in the absence (control) and presence of 1 μ M SPM. Currents were measured at the end of the test pulses and normalized to the amplitude of the current recorded at -140 mV in control conditions. (C) Superimposed Kir4.1/Kir5.1 current traces from A illustrating control currents (black traces) and their respective SPM-induced block (red traces) at +40, +60, +80, and +100 mV. (D) Time constants (τ_{slow} [τ_s] and τ_{fast} [τ_f]) of Kir4.1/Kir5.1 currents as shown in C, in control conditions and in the presence of 1 μ M SPM. (E and F) Current recordings (E) and normalized I-V relationships (F) for Kir4.1 in control and after 1 μ M SPM, obtained as described for A and B, respectively. The dashed line denotes the zero-current level. Data are presented as mean \pm SEM. $n = 5$ for Kir4.1/Kir5.1 and $n = 11$ for Kir4.1. *, $P = 0.047$; +, $P = 0.032$; x, $P = 0.029$.

rectification of Kir4.1/Kir5.1 channels is determined by the flux of K^+ ; that is, it is directly modified according to the direction and magnitude of the K^+ -flux.

Importantly, the intrinsic inward rectification is even evident when applying the slightest depolarization from negative voltages (for instance, stepping to -120 mV following a prepulse of -140 mV; Fig. 7, A and B) as a consequence of partial current deactivation. Measuring currents at the start of the test pulses, the I-V relationship displayed a linear behavior (Fig. 7 B, black squares), reflecting the changes in amplitude dictated by the driving force. However, after this initial jump (instantaneous currents), currents gradually

decreased in a time- and voltage-dependent manner (Fig. 7 A), generating the intrinsic inward rectification of Kir4.1/Kir5.1 (Fig. 7 B, red circles). We quantified the voltage dependence of Kir4.1/Kir5.1 by plotting the relationship between the fraction of open channels ($I_{\text{end}}/I_{\text{start}}$) and the test potential. For the test pulse to -140 mV, the current ratio had a value of ~ 1.0 , indicating that the same fraction of channels remained open during the pulse. In subsequent pulses, the current ratio steeply decreased with membrane depolarization (Fig. 7 C) as a consequence of the channel deactivation. These results reinforce the idea that the K^+ -flux is the determining factor of the intrinsic rectification process.

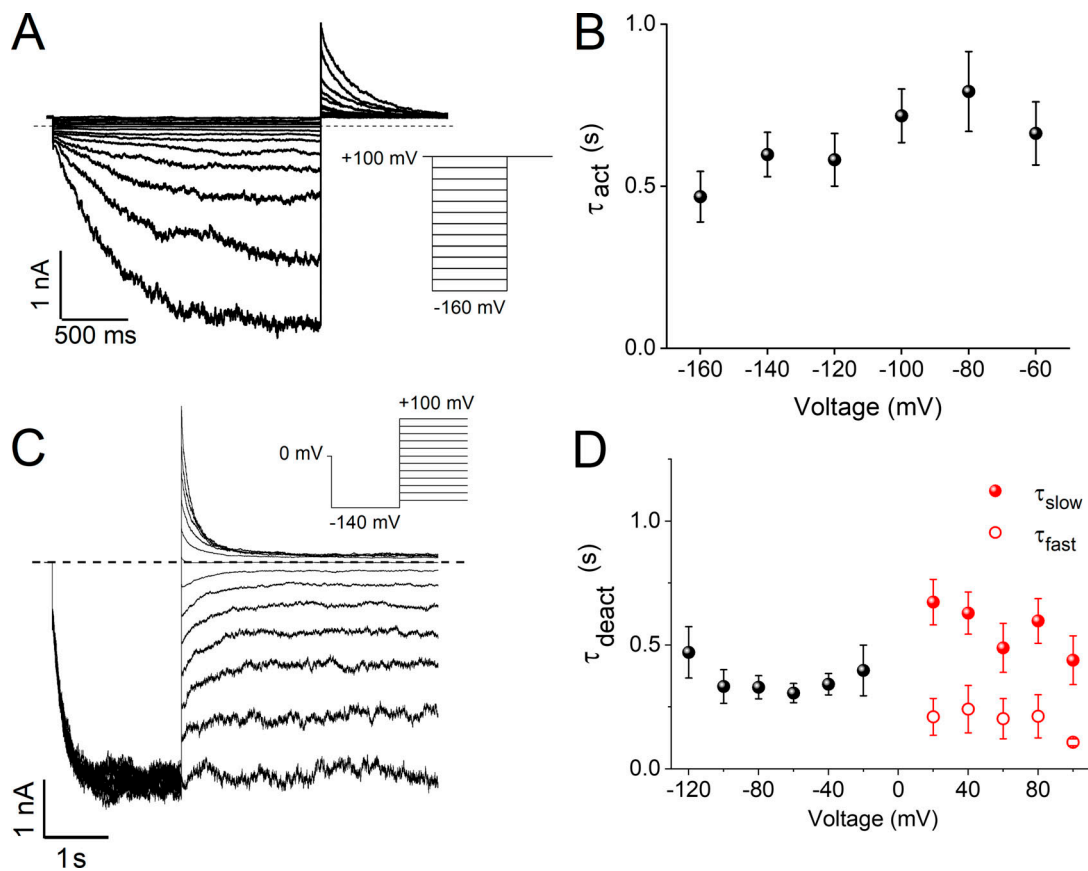


Figure 4. **Voltage-independent activation and deactivation kinetics of Kir4.1/Kir5.1 channels.** (A and C) Inside-out Kir4.1/Kir5.1 current traces elicited with the voltage-step protocols (see insets), which are described in the text and designed for activation (A) or deactivation (C) of currents. (B and D) Time constants of the activation (τ_{act} ; B) and deactivation (τ_{deact} ; D) of Kir4.1/Kir5.1 currents as a function of the test pulse potential. Time constants in black and red were obtained with single and double exponential functions, respectively. The dashed line denotes the zero-current level. Data are presented as mean \pm SEM. $n = 8$ for activation and $n = 6$ for deactivation.

Discussion

From the time of the initial description of inward rectification of K^+ conductance (Katz, 1949), it took until the late 1980s and mid-1990s, when intracellular Mg^{2+} and polyamines were demonstrated to induce the rectification of Kir channels by their voltage-dependent interaction with negative residues facing the inner cavity of these channels (Vandenberg, 1987; Fakler et al., 1994; Lopatin et al., 1994). Later, a weak intrinsic inward rectification was reported despite the use of Mg^{2+} and polyamine-free solutions (Aleksandrov et al., 1996; Shieh et al., 1996; Lee et al., 1999), but it was rapidly found to be caused by trace contaminants in commonly used buffers (Guo and Lu, 2000, 2002). Nevertheless, data supporting a weak intrinsic rectification mechanism in Kir2.1 channels have been reported (Sigg et al., 2018).

In this study, we show that Kir4.1/Kir5.1 channels possess a bona fide strong intrinsic rectification mechanism. The intrinsic inwardly rectifying nature of heteromeric Kir4.1/Kir5.1 channels is supported by (1) the effective washout of intracellular Kir blocking components (Mg^{2+} and polyamines; see Fig. 2 and text); (2) recording solutions that included a phosphate buffer previously demonstrated to contain no impurities with Kir blocking effect (Guo and Lu, 2000, 2002); and (3) the absence of

rectification of homomeric Kir4.1 channels recorded under the same experimental conditions. Additionally, the concomitant voltage-dependent effect of exogenous SPM ($1 \mu M$) on Kir4.1/Kir5.1 outward currents implies that the mechanism of intrinsic rectification coexists with the well-known mechanism of extrinsic rectification produced by Mg^{2+} and polyamines. Furthermore, we provide evidence that the intrinsic rectification mechanism is due to a noncanonical voltage-dependent behavior that operates the gate of this channel.

Gating of Kir channels is thought to involve conformational rearrangements in the cytoplasmic domains in response to diverse stimuli (e.g., G proteins, phosphoinositides, intracellular Na^+ , protons, ATP), ultimately opening or closing the helix-bundle crossing gate (Hansen et al., 2011; Whorton and MacKinnon, 2013; Meng et al., 2016; Nanazashvili et al., 2018). However, no studies have reported changes in membrane voltage as stimuli for Kir channel gating. In fact, Kir4.1/Kir5.1 do not possess a canonical voltage-sensor domain like voltage-gated ion channels, suggesting the existence of an alternative mechanism of voltage sensing. Indeed, the voltage dependence of the activation and deactivation kinetics of Kir4.1/Kir5.1 channels did not exhibit the typical behavior of voltage-gated channels (Fig. 4), a property also reported for the voltage sensor-less Kir6.2(L157E)

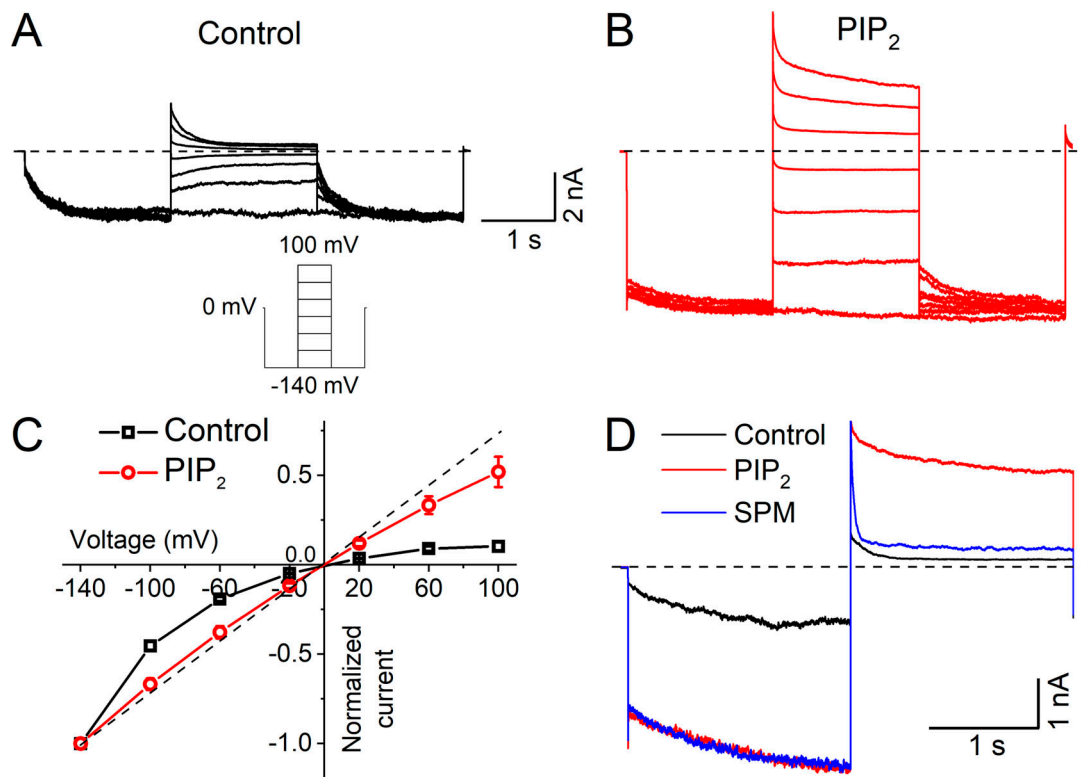


Figure 5. **Exogenous PIP₂ largely reduces the inward rectification of Kir4.1/Kir5.1 channels.** (A and B) Representative Kir4.1/Kir5.1 current traces elicited by the voltage protocol shown at the bottom of A, in control conditions (A) and in the presence of 10 μM PIP₂ (B). (C) Normalized I-V relationships for currents measured at the end of the test pulses, before and after PIP₂ perfusion (*n* = 7). Currents were normalized to that obtained at -140 mV. For comparison, an ohmic behavior is depicted by a dashed line. (D) Superimposed Kir4.1/Kir5.1 current recordings in the presence of 10 μM PIP₂ and after adding 10 μM SPM (similar results were obtained in four more cells). Currents were elicited to -140 mV for 2 s previous to a depolarizing pulse (2 s) to +100 mV (holding potential = 0 mV). The horizontal dashed lines denote the zero-current level.

mutant channel (Kurata et al., 2010). Interestingly, application of exogenous PIP₂ greatly reduced the voltage-gating behavior of Kir4.1/Kir5.1, hence largely decreasing the intrinsic inward rectification. It is known that PIP₂ opens the Kir4.1/Kir5.1 channel at the helix-bundle crossing gate by disrupting a hydrogen bond formed between amino acids from the TM1 and TM2 helices, which stabilizes the closed conformation of the channel (Rapedius et al., 2007). Consequently, the loss of voltage gating after application of a saturating PIP₂ concentration can be explained because the maximal activation of channels has been achieved, suggesting that both stimuli converge at the same physical gate (i.e., the helix-bundle crossing gate).

Previous studies have reported voltage-dependent gating in voltage sensor-less ion channels, including most of the members of the K2P channel family (Schewe et al., 2016), Kir6.2(L157E) and Kir6.2(F168E) mutant channels (Kurata et al., 2010; Vilin et al., 2013), and ClC chloride channels (Chen and Miller, 1996; De Jesús-Pérez et al., 2016). These studies all emphasize the importance of the impact the permeating ion has on the voltage-gating behavior of these ion channels. We observed a similar phenomenon in Kir4.1/Kir5.1 channels, where the I-V relationships underwent parallel shifts when E_K was modified by changing the intracellular or extracellular K⁺ concentration. Moreover, the ion occupancy of the inner cavity seems to have an influence on gating, as reducing intracellular K⁺ (from 200 to

77 or 19 mM) decreased the current ratio. These outcomes reinforce the notion that the gating of Kir4.1/Kir5.1 is not due to voltage-induced conformational changes of the channel protein; rather, they strongly suggest that the gating is driven by the K⁺-flux (Kurata et al., 2010; Schewe et al., 2016). Another characteristic observed when changing ionic gradient conditions was the apparent variation in current kinetics, although this issue deserves a more detailed exploration in future experiments.

In contrast to the Mg²⁺- and polyamine-induced rectification, which primarily occurs at voltages positive to E_K, a notable feature of the intrinsic inward rectification of Kir4.1/Kir5.1 channels is that it arises from voltages negative to E_K (inward currents). This behavior can be explained by a K⁺-flux gating mechanism, according to the following hypothetical model (Fig. 7 D): under symmetrical K⁺ concentrations, there is no net K⁺-flux at a holding potential of 0 mV. Membrane hyperpolarization to -140 mV generates a high inward K⁺-flux, which induces a time-dependent opening of the channel (activation). From this voltage, depolarizing to -100 mV induces a decrease in the instantaneous current amplitude (because of the diminished driving force) and an additional time-dependent reduction originated by the partial deactivation of the channel (either because the gate partially closes or by a decrease in the channel open probability) due to the lowered inward K⁺-flux (Fig. 7 D, top). Contrarily, the outward K⁺-flux is unable to maintain an

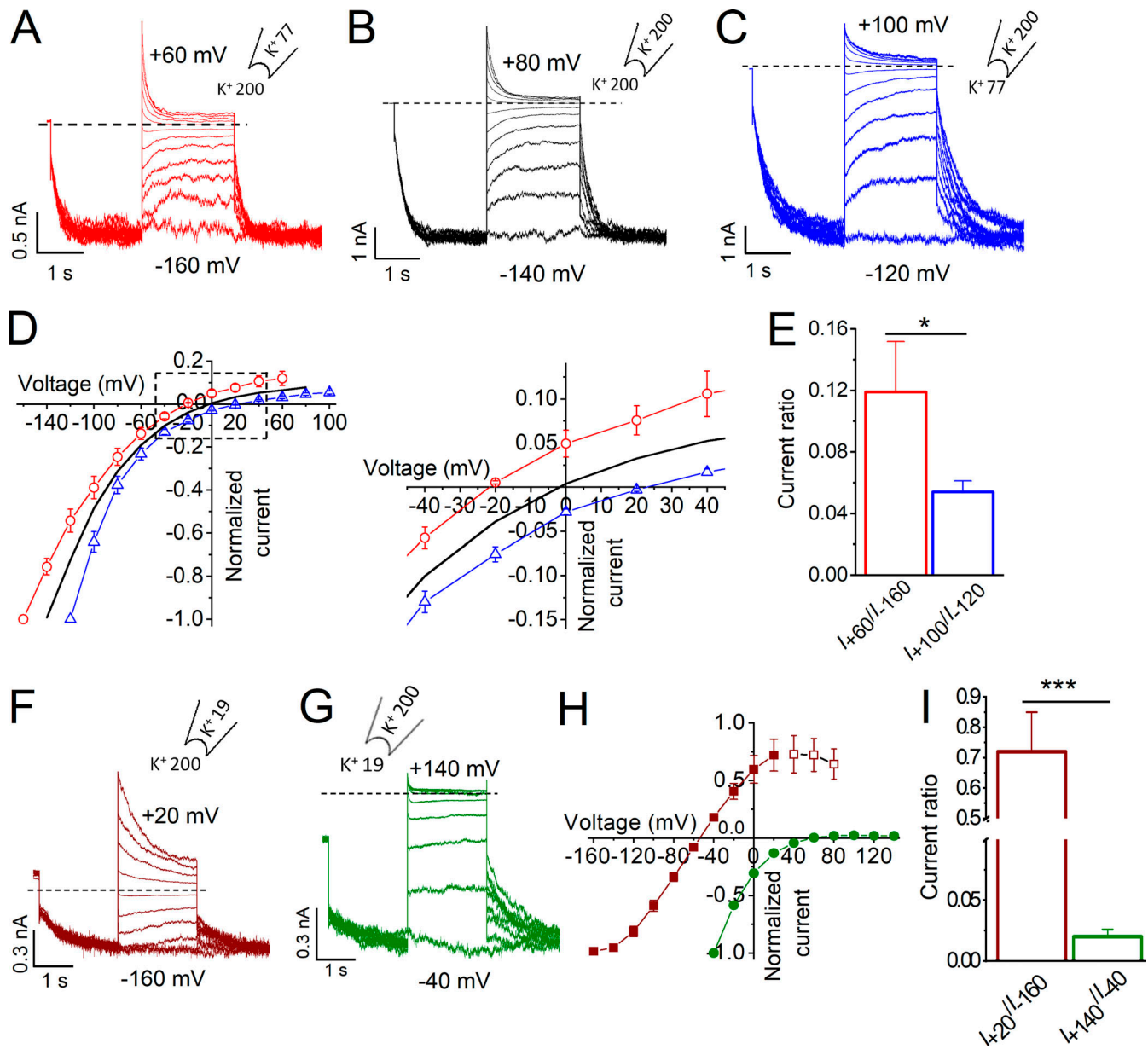


Figure 6. **Effect of asymmetrical K⁺ gradient (200 versus 77 mM and 200 versus 19 mM) on Kir4.1/Kir5.1 I-V relationships. (A–C, F, and G)** Inside-out current traces from Kir4.1/Kir5.1 channels obtained using solutions containing the indicated K⁺ concentration. Currents were induced by voltage protocols as described in the text. **(D and H)** Normalized I–V relationships for currents evoked under conditions displayed in A (red circles), B (black line), C (blue triangles), F (maroon squares), and G (green circles). Note: Three additional test pulses are shown in H (empty maroon squares) to illustrate the persistence of the inward rectification. Current amplitudes were measured at the end of the test pulses and normalized to the respective maximum value at each condition. Current traces in B are those from Fig. 2, which are only shown for comparison purposes, as well as the respective I–V relationship (continuous line in D). The inset at the right of D refers to the amplification of the area delimited in the box. **(E and I)** Current ratios for those obtained at the more depolarized and hyperpolarized potentials under the K⁺ concentration shown in A (red bar), C (blue bar), F (maroon bar), and G (green bar) measuring currents at the end of the test pulses. The dashed line denotes the zero-current level. Data are presented as mean ± SEM. n = 5–6 for all assayed conditions. *, P = 0.048; ***, P = 0.0002.

open gate (Fig. 7 D, bottom); thus, at voltages positive to E_K currents, it falls to almost the zero-current level, generating the strong inward rectification. Interestingly, decreasing the extracellular K⁺ concentration (i.e., increasing the outwardly directed K⁺ gradient) lessens current deactivation, thereby decreasing inward rectification (Fig. 6). This feature could explain the weaker rectification observed in whole-cell (140 K⁺_{int}/4 mM K⁺_{ext}; Fig. 1 B) compared with inside-out (200 K⁺_{int}/200 mM K⁺_{ext}; Fig. 2 B) configurations.

Collectively, our data support a model in which the gate opens powered by the influx of K⁺ but closes (partially and depending on the extracellular K⁺ concentration) during K⁺ efflux. This gating mechanism underlies the strong intrinsic inward rectification of Kir4.1/Kir5.1 channels.

Kir4.1/Kir5.1 heterotetramers are mostly expressed in renal epithelia and glia (Hibino et al., 2010). The K⁺-flux gating mechanism of Kir4.1/Kir5.1 could be relevant for astrocytes, where this channel permits the influx of K⁺ as its concentration

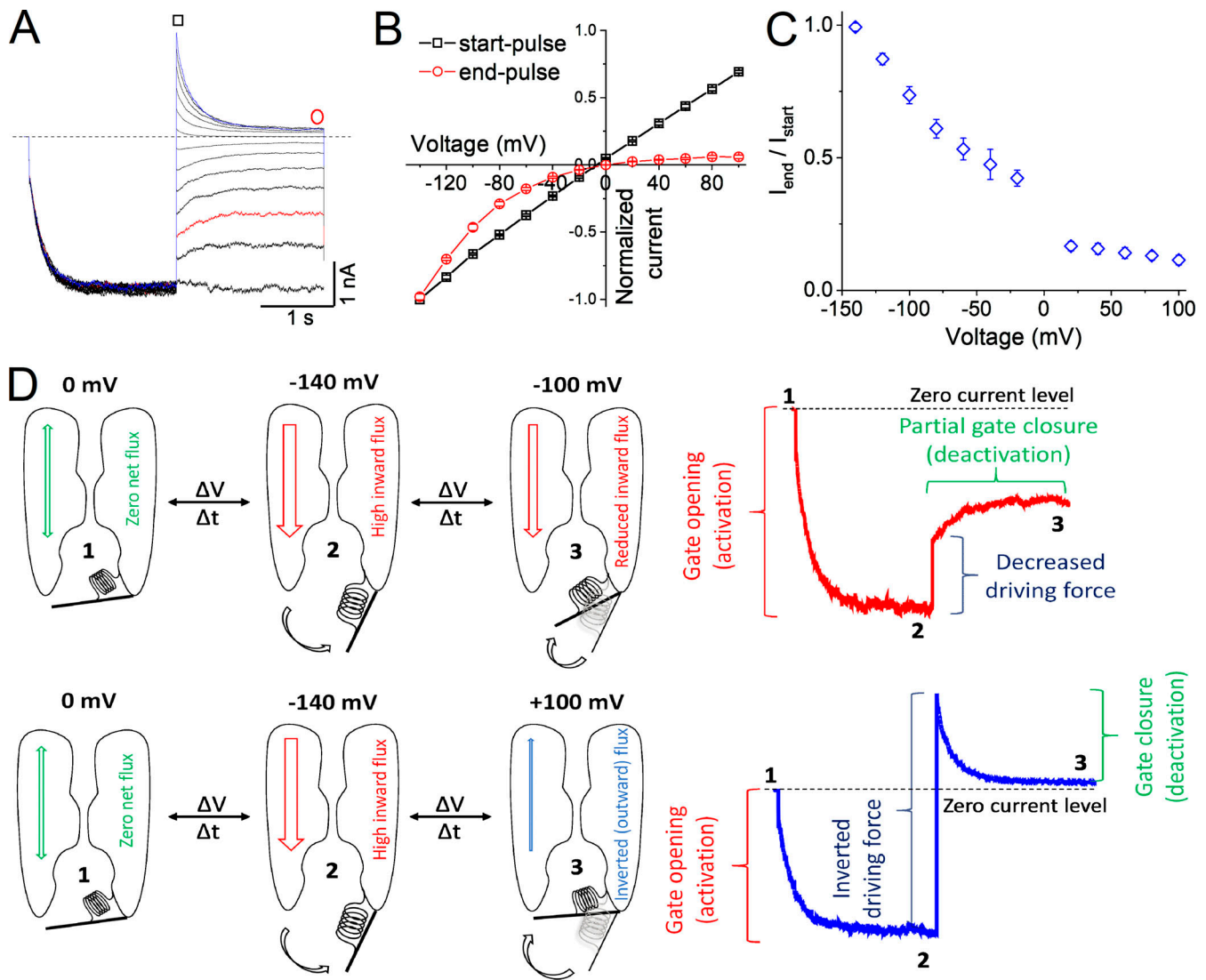


Figure 7. **Gating model for Kir4.1/Kir5.1 channel.** (A) Representative Kir4.1/Kir5.1 currents as described for Fig. 2. The red and blue traces display the currents when the test pulses were -100 and $+100$ mV, respectively (which are shown at the right of D to illustrate the channel gating behavior). (B) Normalized I-V relationships measured at the start and at the end of the test pulses and normalized to the amplitude of the current recorded at -140 mV. (C) Ratio I_{end}/I_{start} as a function of the test pulse potentials. $n = 8$ cells. (D) Hypothetical model of the Kir4.1/Kir5.1 gating mechanism operated by the K^+ -flux. For clarity, two of the four channel subunits are depicted with the ion permeation path between them. The channel activation gate is represented by a hinge. According to the model, inward currents elicited by hyperpolarizing pulses induce the opening of the gate, whereas depolarizing pulses deactivate (to varying degrees) the channel. The partial deactivation of the channels observed at voltages negative to E_K could be either because the gate partially closes or due to a decrease in the channel open probability. Please see a detailed explanation of the hypothetical model in the Discussion section.

increases by neuronal activity, a process called K^+ spatial buffering, which is important for transferring this ion from areas where it is highly concentrated into regions with lower K^+ concentration (Bellot-Saez et al., 2017). The inwardly directed electrochemical K^+ gradient would induce Kir4.1/Kir5.1 opening to remove K^+ from the extracellular space and avoid neuronal hyperexcitability.

Acknowledgments

Merritt Maduke served as editor.

The authors wish to thank Miguel Ángel Flores Virgen (Centro Universitario de Investigaciones Biomédicas, Universidad de

Colima, Colima, México) and Xóchitl Ordaz Ruiz (Facultad de Medicina, Universidad Autónoma de San Luis Potosí, San Luis Potosí, México) for their technical assistance.

This work was partially supported by grants from Secretaría de Educación Pública–Consejo Nacional de Ciencia y Tecnología to J.A. Sánchez-Chapula (CB-2013-01-220546) and A.A. Rodríguez-Menchaca (CB-2016-01-284443) and from Consejo Nacional de Ciencia y Tecnología–Fronteras de la Ciencia to I.A. Aréchiga-Figueroa and A.A. Rodríguez-Menchaca (2016-01-1995).

The authors declare no competing financial interests.

Author contributions: E.G. Moreno-Galindo, T. Ferrer, R.A. Navarro-Polanco, J.A. Sánchez-Chapula, and A.A. Rodríguez-Menchaca designed research; L.G. Marmolejo-Murillo, I.A.

Aréchiga-Figueroa, R. Zamora-Cárdenas, and A.A. Rodríguez-Menchaca performed research; E.G. Moreno-Galindo, T. Ferrer, R.A. Navarro-Polanco, J.A. Sánchez-Chapula, and A.A. Rodríguez-Menchaca contributed new reagents/analytic tools; L.G. Marmolejo-Murillo, I.A. Aréchiga-Figueroa, E.G. Moreno-Galindo, R. Zamora-Cárdenas, and A.A. Rodríguez-Menchaca analyzed data; and E.G. Moreno-Galindo, T. Ferrer, R.A. Navarro-Polanco, and A.A. Rodríguez-Menchaca wrote the paper.

Submitted: 21 November 2019

Revised: 10 November 2020

Accepted: 16 March 2021

References

- Aleksandrov, A., B. Velimirovic, and D.E. Clapham. 1996. Inward rectification of the IRK1 K⁺ channel reconstituted in lipid bilayers. *Biophys. J.* 70: 2680–2687. [https://doi.org/10.1016/S0006-3495\(96\)79837-5](https://doi.org/10.1016/S0006-3495(96)79837-5)
- Bellot-Saez, A., O. Kékesi, J.W. Morley, and Y. Buskila. 2017. Astrocytic modulation of neuronal excitability through K⁺ spatial buffering. *Neurosci. Biobehav. Rev.* 77:87–97. <https://doi.org/10.1016/j.neubiorev.2017.03.002>
- Chen, T.Y., and C. Miller. 1996. Nonequilibrium gating and voltage dependence of the ClC-0 Cl⁻ channel. *J. Gen. Physiol.* 108:237–250. <https://doi.org/10.1085/jgp.108.4.237>
- De Jesús-Pérez, J.J., A. Castro-Chong, R.C. Shieh, C.Y. Hernández-Carballo, J.A. De Santiago-Castillo, and J. Arreola. 2016. Gating the glutamate gate of CLC-2 chloride channel by pore occupancy. *J. Gen. Physiol.* 147:25–37. <https://doi.org/10.1085/jgp.201511424>
- Fakler, B., U. Brändle, C. Bond, E. Glowatzki, C. König, J.P. Adelman, H.P. Zenner, and J.P. Ruppersberg. 1994. A structural determinant of differential sensitivity of cloned inward rectifier K⁺ channels to intracellular spermine. *FEBS Lett.* 356:199–203. [https://doi.org/10.1016/0014-5793\(94\)01258-X](https://doi.org/10.1016/0014-5793(94)01258-X)
- Guo, D., and Z. Lu. 2000. Pore block versus intrinsic gating in the mechanism of inward rectification in strongly rectifying IRK1 channels. *J. Gen. Physiol.* 116:561–568. <https://doi.org/10.1085/jgp.116.4.561>
- Guo, D., and Z. Lu. 2002. IRK1 inward rectifier K⁺ channels exhibit no intrinsic rectification. *J. Gen. Physiol.* 120:539–551. <https://doi.org/10.1085/jgp.20028623>
- Hamill, O.P., A. Marty, E. Neher, B. Sakmann, and F.J. Sigworth. 1981. Improved patch-clamp techniques for high-resolution current recording from cells and cell-free membrane patches. *Pflugers Arch.* 391:85–100. <https://doi.org/10.1007/BF00656997>
- Hansen, S.B., X. Tao, and R. MacKinnon. 2011. Structural basis of PIP2 activation of the classical inward rectifier K⁺ channel Kir2.2. *Nature.* 477: 495–498. <https://doi.org/10.1038/nature10370>
- Hibino, H., A. Inanobe, K. Furutani, S. Murakami, I. Findlay, and Y. Kurachi. 2010. Inwardly rectifying potassium channels: their structure, function, and physiological roles. *Physiol. Rev.* 90:291–366. <https://doi.org/10.1152/physrev.00021.2009>
- Huang, C.L., S. Feng, and D.W. Hilgemann. 1998. Direct activation of inward rectifier potassium channels by PIP2 and its stabilization by Gβγ. *Nature.* 391:803–806. <https://doi.org/10.1038/35882>
- Katz, B. 1949. Les constantes électriques de la membrane du muscle. *Arch. Sci. Physiol. (Paris).* 2:285–289.
- Kubo, Y., and Y. Murata. 2001. Control of rectification and permeation by two distinct sites after the second transmembrane region in Kir2.1 K⁺ channel. *J. Physiol.* 531:645–660. <https://doi.org/10.1111/j.1469-7793.2001.0645h.x>
- Kucheryavykh, Y.V., Y.M. Shuba, S.M. Antonov, M.Y. Inyushin, L. Cubano, W.L. Pearson, H. Kurata, A. Reichenbach, R.W. Veh, C.G. Nichols, et al. 2008. Complex rectification of Müller cell Kir currents. *Glia.* 56: 775–790. <https://doi.org/10.1002/glia.20652>
- Kurata, H.T., M. Rapedius, M.J. Kleinman, T. Baukrowitz, and C.G. Nichols. 2010. Voltage-dependent gating in a “voltage sensor-less” ion channel. *PLoS Biol.* 8:e1000315. <https://doi.org/10.1371/journal.pbio.1000315>
- Lee, J.K., S.A. John, and J.N. Weiss. 1999. Novel gating mechanism of polyamine block in the strong inward rectifier K channel Kir2.1. *J. Gen. Physiol.* 113:555–564. <https://doi.org/10.1085/jgp.113.4.555>
- Lopatin, A.N., E.N. Makhina, and C.G. Nichols. 1994. Potassium channel block by cytoplasmic polyamines as the mechanism of intrinsic rectification. *Nature.* 372:366–369. <https://doi.org/10.1038/372366a0>
- Lu, Z., and R. MacKinnon. 1994. Electrostatic tuning of Mg²⁺ affinity in an inward-rectifier K⁺ channel. *Nature.* 371:243–246. <https://doi.org/10.1038/371243a0>
- Meng, X.Y., S. Liu, M. Cui, R. Zhou, and D.E. Logothetis. 2016. The molecular mechanism of opening the helix bundle crossing (HBC) gate of a Kir channel. *Sci. Rep.* 6:29399. <https://doi.org/10.1038/srep29399>
- Nanazashvili, M., J.E. Sánchez-Rodríguez, B. Fosque, F. Bezanilla, and H. Sackin. 2018. LRET determination of molecular distances during pH gating of the mammalian inward rectifier Kir1.1b. *Biophys. J.* 114:88–97. <https://doi.org/10.1016/j.bpj.2017.10.044>
- Nichols, C.G., and S.J. Lee. 2018. Polyamines and potassium channels: A 25-year romance. *J. Biol. Chem.* 293:18779–18788. <https://doi.org/10.1074/jbc.TM118.003344>
- Pegan, S., C. Arrabit, W. Zhou, W. Kwiatkowski, A. Collins, P.A. Slesinger, and S. Choe. 2005. Cytoplasmic domain structures of Kir2.1 and Kir3.1 show sites for modulating gating and rectification. *Nat. Neurosci.* 8: 279–287. <https://doi.org/10.1038/nn1411>
- Pessia, M., S.J. Tucker, K. Lee, C.T. Bond, and J.P. Adelman. 1996. Subunit positional effects revealed by novel heteromeric inwardly rectifying K⁺ channels. *EMBO J.* 15:2980–2987. <https://doi.org/10.1002/j.1460-2075.1996.tb00661.x>
- Rapedius, M., J.J. Paynter, P.W. Fowler, L. Shang, M.S. Sansom, S.J. Tucker, and T. Baukrowitz. 2007. Control of pH and PIP2 gating in heteromeric Kir4.1/Kir5.1 channels by H-Bonding at the helix-bundle crossing. *Channels (Austin).* 1:327–330. <https://doi.org/10.4161/chan.5176>
- Schewe, M., E. Nematian-Ardestani, H. Sun, M. Musinszki, S. Cordeiro, G. Bucci, B.L. de Groot, S.J. Tucker, M. Rapedius, and T. Baukrowitz. 2016. A non-canonical voltage-sensing mechanism controls gating in K2P K⁺ channels. *Cell.* 164:937–949. <https://doi.org/10.1016/j.cell.2016.02.002>
- Shieh, R.C., S.A. John, J.K. Lee, and J.N. Weiss. 1996. Inward rectification of the IRK1 channel expressed in *Xenopus* oocytes: Effects of intracellular pH reveal an intrinsic gating mechanism. *J. Physiol.* 494:363–376. <https://doi.org/10.1113/jphysiol.1996.sp021498>
- Sigg, D.M., H.K. Chang, and R.C. Shieh. 2018. Linkage analysis reveals allosteric coupling in Kir2.1 channels. *J. Gen. Physiol.* 150:1541–1553. <https://doi.org/10.1085/jgp.201812127>
- Stanfield, P.R., N.W. Davies, P.A. Shelton, I.A. Khan, W.J. Brammar, N.B. Standen, and E.C. Conley. 1994. The intrinsic gating of inward rectifier K⁺ channels expressed from the murine IRK1 gene depends on voltage, K⁺ and Mg²⁺. *J. Physiol.* 475:1–7. <https://doi.org/10.1113/jphysiol.1994.sp020044>
- Swale, D.R., S.V. Kharade, and J.S. Denton. 2014. Cardiac and renal inward rectifier potassium channel pharmacology: Emerging tools for integrative physiology and therapeutics. *Curr. Opin. Pharmacol.* 15:7–15. <https://doi.org/10.1016/j.coph.2013.11.002>
- Vandenberg, C.A. 1987. Inward rectification of a potassium channel in cardiac ventricular cells depends on internal magnesium ions. *Proc. Natl. Acad. Sci. USA.* 84:2560–2564. <https://doi.org/10.1073/pnas.84.8.2560>
- Vilin, Y.Y., J.J. Nunez, R.Y. Kim, G.R. Dake, and H.T. Kurata. 2013. Paradoxical activation of an inwardly rectifying potassium channel mutant by spermine: “(b)locking” open the bundle crossing gate. *Mol. Pharmacol.* 84:572–581. <https://doi.org/10.1124/mol.113.086603>
- Whorton, M.R., and R. MacKinnon. 2013. X-ray structure of the mammalian GIRK2-βγ G-protein complex. *Nature.* 498:190–197. <https://doi.org/10.1038/nature12241>
- Yang, J., Y.N. Jan, and L.Y. Jan. 1995. Determination of the subunit stoichiometry of an inwardly rectifying potassium channel. *Neuron.* 15: 1441–1447. [https://doi.org/10.1016/0896-6273\(95\)90021-7](https://doi.org/10.1016/0896-6273(95)90021-7)